Contrib. Astron. Obs. Skalnaté Pleso **49**, 7 – 18, (2019)

Estimating the black hole mass of NGC 1313 X-1 based on the spectral and timing properties

C.-Y. Huang

School of Physics and Optoelectronic Engineering, Yangtze University, Jingzhou 434023, China (E-mail: hcy@yangtzeu.edu.cn)

Received: September 26, 2018; Accepted: November 15, 2018

Abstract. The discovery of 3:2 quasi-periodic oscillations (QPOs) in the ultra-luminous X-ray source NGC 1313 X-1 suggests it harbors an intermediate-mass black hole (IMBH). We test this numerically by modelling the 3:2 QPOs and the associated X-ray spectrum based on the epicyclic resonance model and a disk-corona model with large-scale magnetic fields generated by the Cosmic Battery mechanism. The combined QPO-frequency and spectral fitting indicates that the BH mass ranges from $2524M_{\odot}$ to $6811M_{\odot}$ confirming its IMBH nature, and the BH spin is probably higher than ~ 0.3.

Key words: accretion, accretion disks – black hole physics – magnetic fields – stars: individual: NGC 1313 X-1

1. Introduction

Ultraluminous X-ray sources (ULXs) are non-nuclear point-like X-ray sources in nearby galaxies with luminosities greater than $\sim 10^{39}$erg s^{-1}. The nature of the compact objects in ULXs is still under debate. They are generally thought to be powered by the intermediate-mass (10^2 – $10^4 M_{\odot}$) black holes (IMBHs) since the luminosity exceeds the Eddington limit for a typical stellar-mass ($\sim 10M_{\odot}$) black hole (BH), where $M_{\odot}$ is the solar mass. However, the spectral analyses based on high quality observations indicate that they may harbor stellar-mass BHs accreting at near-Eddington or super-Eddington rate (e.g. Stobbart et al., 2006; Gladstone et al., 2009; Jithesh et al., 2017). The super-Eddington phenomenon could also be explained by the beaming geometry or the relativistic beaming of jet emission (e.g. King et al., 2001; Poutanen et al., 2007; Körding et al., 2002; Freeland et al., 2006; Kuncic et al., 2007). Recently, the discovery of coherent X-ray pulsations from some ULXs indicates that the central engines are accreting neutron stars (Bachetti et al., 2014; Israel et al., 2017b; Fürst et al., 2016; Israel et al., 2017a; Koliopanos et al., 2017). See Kaaret et al. (2017) for a review. A direct mass measurement is needed to clarify the question of what are the compact objects harbored in ULXs.

Timing properties provide us an important clue to constrain the mass and spin of the compact objects. The discovery of 3:2 quasi-periodic oscillation (QPO) pairs in two ULXs indicates that they harbor IMBHs. Pasham et al. (2014) reported a 3:2 QPO pair at frequencies 5 and 3.3 Hz detected in ULX

M82 X-1 and estimated the mass of the compact object to be $428 \pm 105 M_{\odot}$ using the inverse correlation between the BH mass and the frequencies of high-frequency QPOs (HFQPOs) observed in galactic BH X-ray binaries (BHXBs). Soon afterwards Pasham et al. (2015) detected another 3:2 QPO pair at frequencies 0.45 and 0.3 Hz in *XMM-Newton* observations of ULX NGC 1313 X-1. They found that the power density spectrum of NGC 1313 X-1 is analogous to that of BHXBs in the steep power-law (SPL) state and estimated the BH mass to be $5000 M_{\odot}$ using the inverse mass-to-HFQPO frequency scaling.

Jang et al. (2018) applied the X-ray scaling method to measure the BH mass in ULXs with multiple X-ray observations and their estimated BH mass of NGC 1313 X-1 was in the range 295 – 6166 $M_{\odot}$.

Both the QPO scaling and the X-ray scaling methods imply NGC 1313 X-1 harbors an IMBH. However, quantitative and numerical analyses are needed to test this result. In this paper, we estimate the BH mass in NGC 1313 X-1 by modelling the 3:2 QPOs and the associated X-ray spectrum simultaneously based on the epicyclic resonance model (ERM) and a magnetic disk-corona model developed by Huang et al. (2016).

The paper is organised as follows. In section 2, we give a description of the model. In section 3, the 3:2 QPO frequencies and the associated X-ray spectrum are fitted and the range of the BH mass is obtained. We discuss and summarize in section 4. The geometric units $G = c = 1$ are used throughout this paper.

2. Model description

2.1. The magnetic disk-corona model

The energy transferred from the rotating BH and the plunging region to the inner disk is considered through the magnetic connection (MC) process by the large-scale magnetic fields generated by the Poynting-Robertson Cosmic Battery (PRCB) mechanism (Contopoulos & Kazanas, 1998; Contopoulos et al., 2006; Kylafis et al., 2012). In the PRCB scenario, electrons in the inner accretion disk feel a much stronger radiation-drag force than the ions due to a much larger Thompson cross-section leading to an electric current loop generated near the inner edge of the accretion disk. The current intensity can be estimated as (Huang et al., 2016)

$$I = en\Delta t \Delta S F \sigma_{\rm T} v_{\rm k}/m_{\rm e}, \tag{1}$$

where Δt and ΔS are the average scattering time of electrons with photons and the cross-section of the current, respectively, F is the radiation flux from the relativistic accretion disk (Novikov & Thorne, 1973; Page & Thorne, 1974), n is the number density of electrons, $v_{\rm k}$ is the Kepler velocity, $\sigma_{\rm T}$ is the Thompson cross-section and e is the electric quality of an electron. Following Huang et al. (2016), we set $\Delta t = 10^{-9}$s and $\Delta S = (0.01 M_{\rm BH})^2$, where $M_{\rm BH}$ is the BH mass. The values of F, n and $v_{\rm k}$ are all evaluated at the radius $r_{\rm PRCB}$ where

the current is generated. As suggested by Kylafis et al. (2012), the current is generated near the innermost stable circular orbit (ISCO) of the disk. Fitting the 3:2 HFQPO pairs and the associated spectrum from BHXBs by Huang et al. (2016) also indicates that the current is very near the ISCO. For simplicity, We set $r_{\rm PRCB} = 1.01 r_{\rm ISCO}$ in this work, where $r_{\rm ISCO}$ is the radius of ISCO.

The magnetic fields generated by the PRCB current can be calculated in the frame of general relativity (Linet, 1979; Li, 2002b). As shown in Huang et al. (2016), two types of MC configurations are created by the PRCB current with one connecting the BH horizon and the disk and the other connecting the plunging region and the inner disk. The rotational energy of both the BH and the plunging region can be transferred to the inner disk by these two MC processes. The energy dissipated at unit disk area caused by MC is expressed as (Li, 2002a)

$$Q^{+}_{\rm MC} = r^{-1} S^{-2} (-\frac{{\rm d}\Omega_{\rm D}}{{\rm d}r}) \int_{r_{\rm in}}^{r} S H_{\rm MC} r {\rm d}r, \tag{2}$$

where $S = E^{\dagger} - \Omega_{\rm D} L^{\dagger}$ with $E^{\dagger}$, $L^{\dagger}$ and $\Omega_{\rm D}$ are, respectively, the specific energy, the specific angular momentum and angular velocity of a test particle in the accretion disk (Bardeen et al., 1972). In equation (2), $H_{\rm MC} \equiv \frac{1}{4\pi r}\frac{{\rm d}T}{{\rm d}r}$ is the flux of angular momentum transferred to the disk, where T is the torque exerting on the disk surface by MC (Li, 2002a), and $r_{\rm in}$ is the inner most disk radius receiving energy from the plunging region.

The gravitational power dissipated in unit disk surface is (Page & Thorne, 1974)

$$Q^{+}_{\rm DA} = \frac{\dot{M}}{4\pi r} f, \tag{3}$$

where $\dot{M}$ is the mass accretion rate of the disk and f is a function of a_*, r and $M_{\rm BH}$ as given in Page & Thorne (1974), where $a_* \equiv J/M^2_{\rm BH}$ is the dimensionless BH spin defined in terms of $M_{\rm BH}$ and BH angular momentum J.

The corona is assumed to be heated by the reconnection of the small-scale magnetic field that generated by the buoyancy instability in the disk (Di Matteo, 1998; Liu et al., 2002). The power dissipated in the corona is (Liu et al., 2002)

$$Q^{+}_{\rm cor} = \frac{B^2_{\rm d}}{4\pi} v_{\rm A}, \tag{4}$$

where $B_{\rm d}$ is the small-scale magnetic field in the disk, and $v_{\rm A} \equiv B_{\rm d}/\sqrt{4\pi\rho}$ is the Alfvén speed, where ρ is the mass density of the disk.

Part of the energy dissipated in the disk is radiated as black body, and the other part is released into the corona. Thus, the energy equation for the disk is

$$Q^{+}_{\rm DA} + Q^{+}_{\rm MC} - Q^{+}_{\rm cor} = \frac{4\sigma T^4_{\rm d}}{3\tau_{\rm d}}, \tag{5}$$

where $T_{\rm d}$ is the temperature in the mid-plane of the disk, σ is the Stefan-Boltzmann constant, and $\tau_{\rm d}$ is the optical depth in the vertical direction of the

disk which is related to the mean opacity κ as

$$\tau_{\rm d} = \rho h \kappa = \rho h(\kappa_{\rm ff} + \kappa_{\rm es}), \tag{6}$$

where h is the half-thickness of the disk, $\kappa_{\rm ff}$ and $\kappa_{\rm es}$ are the contributions of free-free transitions and electron scattering respectively, and $\kappa_{\rm ff} = 6.4 \times 10^{22} \rho T_{\rm d}^{-7/2}\,{\rm cm^2\,g^{-1}}$ and $\kappa_{\rm es} = 0.4\,{\rm cm^2\,g^{-1}}$ are adopted (Novikov & Thorne, 1973).

The equation for the vertical pressure balance of the disk is (Novikov & Thorne, 1973)

$$h = P^{1/2} \rho^{-1/2} r^{3/2} M_{\rm BH}^{-1/2} \mathcal{A}\mathcal{B}^{-1} \mathcal{C}^{1/2} \mathcal{D}^{-1/2} \mathcal{E}^{-1/2}, \tag{7}$$

where $P = P_{\rm gas} + P_{\rm rad} + P_{\rm mag}$, and $P_{\rm gas}$, $P_{\rm rad}$ and $P_{\rm mag}$ are, respectively, the gas pressure, radiation pressure and magnetic pressure of the disk. $\mathcal{A}$, $\mathcal{B}$, $\mathcal{C}$, $\mathcal{D}$ and $\mathcal{E}$ are the relativistic correction factors in Kerr metric (Novikov & Thorne, 1973).

Magnetohydrodynamics (MHD) simulations reveal that the viscosity in the accretion disk is related to the tangled small-scale magnetic fields. However, the detailed physics of the generation of the small-scale magnetic fields is still unclear. The famous 'α-prescription' proposed by Shakura & Sunyaev (1973) is widely used in various theoretical works. Observations favor the interior viscous stress $t_{r\varphi}$ proportional to the gas pressure (Wang et al., 2004). Therefore we adopt this α-prescription in our calculation:

$$t_{r\varphi} = P_{\rm mag} = \frac{B_{\rm d}^2}{8\pi} = \alpha P_{\rm gas}, \tag{8}$$

where α is the viscosity parameter.

The continuity equation of the disk is (Novikov & Thorne, 1973)

$$\dot{M} = -4\pi r h \rho v_r \mathcal{D}^{1/2}, \tag{9}$$

where v_r is the radial velocity of the accretion flow at radius r. Incorporating the energy and angular-momentum equations for the disk, the stress $t_{r\varphi}$ is related to the dissipated energy as follow (Page & Thorne, 1974; Li, 2002a)

$$rht_{r\varphi} = S(-\frac{{\rm d}\Omega_{\rm D}}{{\rm d}r})^{-1}(Q_{\rm DA}^{+} + Q_{\rm MC}^{+}). \tag{10}$$

The equation of state for the gas in the disk is

$$P_{\rm rad} + P_{\rm gas} = \frac{1}{3} a_0 T_{\rm d}^4 + \frac{\rho k T_{\rm d}}{\mu m_{\rm p}}, \tag{11}$$

where a_0 is the radiation constant, k is the Boltzmann constant, $m_{\rm p}$ is the proton mass, and $\mu = 0.615$ is adopted being the mean atomic mass.

The electrons in the corona are heated by the magnetic reconnection and are cooled via the inverse Compton scattering by the soft photons from the cold disk. Thus, the energy equation of the corona is (Liu et al., 2002)

$$Q_{\rm cor}^{+} = Q_{\rm comp}^{-} = \frac{4kT_{\rm e}}{m_{\rm e}}\tau U_{\rm rad}, \tag{12}$$

where $U_{\rm rad} = a_0 T_{\rm d}^4$ is the energy density of the soft photon field, $T_{\rm e}$ is the temperature of the corona, $m_{\rm e}$ is the electron mass, and τ is the optical depth of the corona.

Following Huang et al. (2016), we take the optical depth, the height and the outer boundary of the corona as $\tau = 1$, $l = 20M_{\rm BH}$ and $r_{\rm out} = 100M_{\rm BH}$, respectively. Solving equations (1) – (12) numerically, we can obtain the global solutions of the disk-corona system with MC process. The X-ray spectrum of the system can be simulated using Monte Carlo method (Gan et al., 2009).

2.2. The 3:2 QPO model

There is no consensus on the mechanism of QPO generation although a variety of models have been proposed (see Belloni & Stella, 2014, for a review). We interpret 3:2 QPO pairs based on ERM (Abramowicz & Kluźniak, 2001) since it naturally explains the small integer ratios of 3:2 QPO frequencies.

In the general relativistic frame, a test particle in the equatorial plane around a compact object has three basic oscillation frequencies, namely, the orbital frequency ν_ϕ, the vertical epicyclic frequency ν_θ and the radial epicyclic frequency ν_r, which are functions of a_*, r and $M_{\rm BH}$ given as follows (Bardeen et al., 1972; Okazaki et al., 1987; Kato, 1990; van der Klis, 2006)

$$\nu_\phi = [2\pi M_{\rm BH}(\tilde{r}^{3/2} + a_*)]^{-1}, \tag{13}$$

$$\nu_\theta = \nu_\phi(1 - 4a_*\tilde{r}^{-3/2} + 3a_*^2\tilde{r}^{-2})^{1/2}, \tag{14}$$

$$\nu_r = \nu_\phi(1 - 6\tilde{r}^{-1} + 8a_*\tilde{r}^{-3/2} - 3a_*^2\tilde{r}^{-2})^{1/2}, \tag{15}$$

where $\tilde{r} \equiv r/M_{\rm BH}$.

In ERM, resonances occur at specific radii of the disk if the vertical and the radial epicyclic frequencies have small integer ratios resulting in oscillations of the plasmoid. As argued by Huang et al. (2010, 2016), the severe damping forces on the oscillations can be overcome by transferring energy from the spinning BH to the inner disk via the MC process therefore the resonances persist and emit X-rays with sufficient amplitude and coherence to produce the observed QPOs.

Applying to NGC 1313 X-1, we treat the frequency of the 0.45 Hz QPO as ν_θ and the 0.3 Hz as ν_r. For a given BH spin, the BH mass and the resonance radius $\tilde{r}_{\rm res}$ can be obtained by solving the equations

$$\begin{cases} \nu_\theta/\nu_r = 3/2, \\ \nu_\theta = 0.45. \end{cases} \tag{16}$$

Table 1. Parameters for fitting the 3:2 QPO frequencies and the associated X-ray spectrum.

a_*	$m_{\rm BH}$	$\tilde{r}_{\rm res}$	$\dot{m}$	α	$n_{\rm H}(10^{22}{\rm cm}^{-2})$
0.3	2524	9.13	0.38	0.39	0.45
0.998	6811	3.89	0.00032	0.22	0.28

3. Fitting the 3:2 QPO frequencies and the associated X-ray spectrum

The 0.45 and 0.3 Hz QPOs of NGC 1313 X-1 were detected simultaneously on 2012 December 16 in the *XMM-Newton* observation (obsID: 0693850501) at energy band of 0.3 – 10 keV (Pasham et al., 2015). We first fit the 3:2 QPO frequencies and then fit the 0.3 – 10 keV spectrum from this *XMM-Newton* observation.

In the spectral simulation, the distance to the source $d = 4.61$Mpc (Qing et al., 2015) is adopted and the inclination i of the system is assumed to be 70° for an analogy with the X-ray binary systems since almost all the BHXBs displaying HFQPOs have high inclinations (Miller & Miller, 2015), which is close to the values (66° – 76°) obtained by spectral fitting models of Bachetti et al. (2013).

Since the BH spin of NGC 1313 X-1 has not been measured, we consider two extremes, the Schwarzschild BH with $a_* = 0$ and the extreme Kerr BH with $a_* = 0.998$. The corresponding lower and upper limits of the BH mass obtained by solving equation (16) are $2024M_\odot$ and $6811M_\odot$, respectively. Based on the values of $m_{\rm BH}$ ($m_{\rm BH} \equiv M_{\rm BH}/M_\odot$) and a_*, we then fit the spectrum by adjusting the parameters $\dot{m}$, α and $n_{\rm H}$, where $\dot{m} \equiv \dot{M}/\dot{M}_{\rm Edd}$ and $\dot{M}_{\rm Edd} \simeq 1.4 \times 10^{18} m_{\rm BH}$ g s^{-1} is the Eddington accretion rate, and $n_{\rm H}$ is the hydrogen column density.

It turns out that a larger BH mass leads to a better spectral fitting and the spectrum can not be fitted well if $a_* \lesssim 0.3$ since the BH mass is too small. The parameters corresponding to the lower and upper limits of the values of a_* and $m_{\rm BH}$ for fitting the 3:2 QPO frequencies and the associated X-ray spectrum are listed in Table 1. The corresponding simulated spectra are plotted in Fig. 1, which fit very well into the observed one in the 0.5 – 10 keV band. The deviation below 0.5 keV may be due to that we do not consider the synchrotron and bremsstrahlung radiation from the corona in our model.

The simulated spectrum is more sensitive to $\dot{m}$ for a larger a_* due to the stronger MC effect by the large-scale magnetic fields generated by PRCB current which is proportional to $\dot{m}$ as indicated by equation (3).

Inspecting Table 1, one can find that a larger BH mass is needed to fit the 3:2 QPO frequencies for a higher BH spin. And larger values of $\dot{m}$ and α are needed

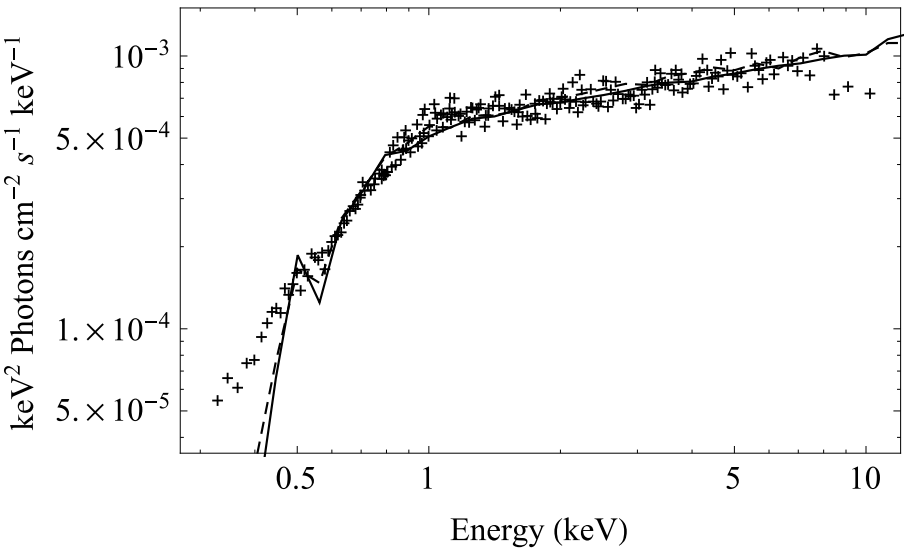

Figure 1. The simulated and observed spectra of NGC 1313 X-1 associated with the 3:2 QPOs. The solid and dashed lines represent the model spectra with $a_* = 0.3$ and $a_* = 0.998$, respectively. The symbol "+" denotes the observed spectrum (without error bars) with data taken from Bachetti et al. (2013).

to fit the spectrum for a lower BH spin and a smaller BH mass, which means both the soft component, which is proportional to $\dot{m}$ as indicated by equation (3), and the hard component, which is proportional to α as indicated by equation (8) and equation (4), should be enhanced to fit the observed spectrum.

4. Summary and discussion

In this paper, we modelled the 0.45 and 0.3 Hz QPOs and the associated 0.3 – 10 keV X-ray spectrum of NGC 1313 X-1 based on ERM and a disk-corona model with PRCB. The combined QPO-frequency and spectral fitting indicates that the BH mass lies in the range $2524 - 6811 M_\odot$ and the BH spin is probably higher than ~ 0.3. This is the first time to model the combined spectral and timing properties of NGC 1313 X-1 numerically and self-consistently. The result confirms that NGC 1313 X-1 contains an IMBH consistent with the results of Pasham et al. (2015) and Jang et al. (2018).

We find that the magnetic fields play an important role in the spectral fitting. The simulated spectra are in accordance with the observed one only when the intensity of the magnetic fields at $r_{\rm ISCO}$ generated by PRCB is comparable to that at the BH horizon evaluated by the balance of the ram pressure and the

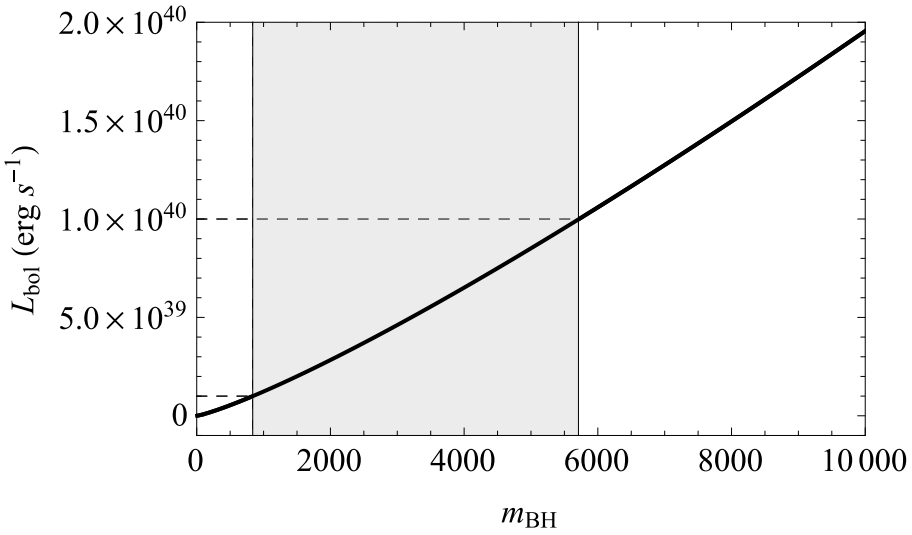

Figure 2. The curve of the bolometric luminosity as a function of BH mass for the PRCB magnetic fields at ISCO become saturated. The shaded area indicates the BH mass ranges between $839M_\odot$ and $5719M_\odot$ for the bolometric luminosity ranges from 10^{39} to 10^{40} erg s^{-1}.

magnetic pressure. This means that the magnetic fields become saturated and the disk is in the magnetically arrested disk (MAD) state (Igumenshchev et al., 2003). Our model suggests that ULXs especially those brightest, like NGC 1313 X-1, may be close to or reach the MAD state. If this is indeed the case, we can predict the bolometric luminosity of an ULX by figuring out the accretion rate to make the magnetic fields become saturated for a given BH mass, or, conversely, the BH mass can be obtained with the saturated magnetic fields for a given bolometric luminosity.

Let's make a simple estimate. For $a_* = 0.9$ and $\alpha = 0.3$, the intensity of the PRCB magnetic fields $B_{\rm PRCB}$ at $r_{\rm ISCO}$ in our model can be expressed as

$$B_{\rm PRCB} = 4.5\times10^7 \left(\frac{\dot{m}}{0.1}\right)^{1.5} \left(\frac{m_{\rm BH}}{5000}\right)^{-0.7} \text{Gauss}. \tag{17}$$

The MAD magnetic fields can be estimated by the balance of the ram pressure of the innermost part of the accretion flow and the magnetic pressure on the BH horizon (Moderski et al., 1997; Wang et al., 2002; Gan et al., 2009):

$$B_{\rm MAD} = \sqrt{2\dot{M}/r_{\rm H}} = 6.1\times10^6 \left(\frac{\dot{m}}{0.1}\right)^{0.5} \left(\frac{m_{\rm BH}}{5000}\right)^{-0.5} \text{Gauss}, \tag{18}$$

where $r_{\rm H} = M_{\rm BH}(1 + \sqrt{1 - a_*^2})$ is the radius of the BH horizon. Assuming the radiation efficiency $\eta = 0.1$ and the bolometric luminosity $L_{\rm bol} = \eta \dot{M}$, let $B_{\rm PRCB} = B_{\rm MAD}$, we have

$$L_{\rm bol} = 8.5 \times 10^{39} \left(\frac{m_{\rm BH}}{5000}\right)^{1.2} {\rm erg\ s^{-1}}. \quad (19)$$

If $L_{\rm bol}$ is between 10^{39} and 10^{40} erg s^{-1}, then the constrained BH mass is between $839 M_\odot$ and $5719 M_\odot$, as indicated by the grey shaded area in Fig. 2.

In the spectral fitting, we only considered the 0.3 – 10 keV *XMM-Newton* spectrum associated with the 3:2 QPOs. The *NuSTAR* spectrum shows a clear cutoff above 10 keV and decays up to $\sim$ 30 keV, which can be described by a phenomenological model that includes a multi-color disk plus a two-component corona composed of a cold, optically thick medium and a second, hot and optically thin one (Bachetti et al., 2013). We will improve our model by considering multi-temperature corona with different geometries (e.g. spherical corona, "lamp-post" corona) in future works to understand both the *XMM-Newton* and *NuSTAR* spectra and to obtain more accurate and reliable measurements for the BH mass and spin of NGC 1313 X-1 and other BH systems.

Acknowledgements. This work has been supported by the National Natural Science Foundation of China (Grant No.11403003). We thank the anonymous referee for his (her) helpful suggestion.

References

Abramowicz, M. A. & Kluźniak, W., A precise determination of black hole spin in GRO J1655-40. 2001, *Astron. Astrophys.*, **374**, L19, DOI: 10.1051/0004-6361:20010791

Bachetti, M., Harrison, F. A., Walton, D. J., et al., An ultraluminous X-ray source powered by an accreting neutron star. 2014, *Nature*, **514**, 202, DOI: 10.1038/nature13791

Bachetti, M., Rana, V., Walton, D. J., et al., The Ultraluminous X-Ray Sources NGC 1313 X-1 and X-2: A Broadband Study with NuSTAR and XMM-Newton. 2013, *Astrophys. J.*, **778**, 163, DOI: 10.1088/0004-637X/778/2/163

Bardeen, J. M., Press, W. H., & Teukolsky, S. A., Rotating Black Holes: Locally Nonrotating Frames, Energy Extraction, and Scalar Synchrotron Radiation. 1972, *Astrophys. J.*, **178**, 347, DOI: 10.1086/151796

Belloni, T. M. & Stella, L., Fast Variability from Black-Hole Binaries. 2014, *Space Sci. Rev.*, **183**, 43, DOI: 10.1007/s11214-014-0076-0

Contopoulos, I. & Kazanas, D., A Cosmic Battery. 1998, *Astrophys. J.*, **508**, 859, DOI: 10.1086/306426

Contopoulos, I., Kazanas, D., & Christodoulou, D. M., The Cosmic Battery Revisited. 2006, *Astrophys. J.*, **652**, 1451, DOI: 10.1086/507600

Di Matteo, T., Magnetic reconnection: flares and coronal heating in active galactic nuclei. 1998, *Mon. Not. R. Astron. Soc.*, **299**, L15, DOI: 10.1046/j.1365-8711.1998.01950.x

Freeland, M., Kuncic, Z., Soria, R., & Bicknell, G. V., Radio and X-ray properties of relativistic beaming models for ultraluminous X-ray sources. 2006, *Mon. Not. R. Astron. Soc.*, **372**, 630, DOI: 10.1111/j.1365-2966.2006.10750.x

Fürst, F., Walton, D. J., Harrison, F. A., et al., Discovery of Coherent Pulsations from the Ultraluminous X-Ray Source NGC 7793 P13. 2016, *Astrophys. J., Lett.*, **831**, L14, DOI: 10.3847/2041-8205/831/2/L14

Gan, Z.-M., Wang, D.-X., & Lei, W.-H., A model of magnetically induced disc-corona for black hole binaries. 2009, *Mon. Not. R. Astron. Soc.*, **394**, 2310, DOI: 10.1111/j.1365-2966.2009.14518.x

Gladstone, J. C., Roberts, T. P., & Done, C., The ultraluminous state. 2009, *Mon. Not. R. Astron. Soc.*, **397**, 1836, DOI: 10.1111/j.1365-2966.2009.15123.x

Huang, C.-Y., Gan, Z.-M., Wang, J.-Z., & Wang, D.-X., A resonance model with magnetic connection for 3:2 HFQPO pairs in black hole binaries. 2010, *Mon. Not. R. Astron. Soc.*, **403**, 1978, DOI: 10.1111/j.1365-2966.2009.16237.x

Huang, C.-Y., Ye, Y.-C., Wang, D.-X., & Li, Y., A model for 3:2 HFQPO pairs in black hole binaries based on cosmic battery. 2016, *Mon. Not. R. Astron. Soc.*, **457**, 3859, DOI: 10.1093/mnras/stw226

Igumenshchev, I. V., Narayan, R., & Abramowicz, M. A., Three-dimensional Magnetohydrodynamic Simulations of Radiatively Inefficient Accretion Flows. 2003, *Astrophys. J.*, **592**, 1042, DOI: 10.1086/375769

Israel, G. L., Belfiore, A., Stella, L., et al., An accreting pulsar with extreme properties drives an ultraluminous x-ray source in NGC 5907. 2017a, *Science*, **355**, 817, DOI: 10.1126/science.aai8635

Israel, G. L., Papitto, A., Esposito, P., et al., Discovery of a 0.42-s pulsar in the ultraluminous X-ray source NGC 7793 P13. 2017b, *Mon. Not. R. Astron. Soc.*, **466**, L48, DOI: 10.1093/mnrasl/slw218

Jang, I., Gliozzi, M., Satyapal, S., & Titarchuk, L., Measuring the black hole mass in ultraluminous X-ray sources with the X-ray scaling method. 2018, *Mon. Not. R. Astron. Soc.*, **473**, 136, DOI: 10.1093/mnras/stx2178

Jithesh, V., Misra, R., & Wang, Z., Long-term Spectral Variability of the Ultraluminous X-Ray Source Holmberg IX X-1. 2017, *Astrophys. J.*, **849**, 121, DOI: 10.3847/1538-4357/aa8eeb

Kaaret, P., Feng, H., & Roberts, T. P., Ultraluminous X-Ray Sources. 2017, *Ann. Rev. Astron. Astrophys.*, **55**, 303, DOI: 10.1146/annurev-astro-091916-055259

Kato, S., Trapped one-armed corrugation waves and QPOs. 1990, *Publ. Astron. Soc. Jap.*, **42**, 99

King, A. R., Davies, M. B., Ward, M. J., Fabbiano, G., & Elvis, M., Ultraluminous X-Ray Sources in External Galaxies. 2001, *Astrophys. J., Lett.*, **552**, L109, DOI: 10.1086/320343

Koliopanos, F., Vasilopoulos, G., Godet, O., et al., ULX spectra revisited: Accreting, highly magnetized neutron stars as the engines of ultraluminous X-ray sources. 2017, *Astron. Astrophys.*, **608**, A47, DOI: 10.1051/0004-6361/201730922

Körding, E., Falcke, H., & Markoff, S., Population X: Are the super-Eddington X-ray sources beamed jets in microblazars or intermediate mass black holes? 2002, *Astron. Astrophys.*, **382**, L13, DOI: 10.1051/0004-6361:20011776

Kuncic, Z., Soria, R., Hung, C. K., Freeland, M. C., & Bicknell, G. V., Ultra-luminous X-ray sources: X-ray binaries in a high/hard state? 2007, in IAU Symposium, Vol. **238**, *Black Holes from Stars to Galaxies – Across the Range of Masses*, ed. V. Karas & G. Matt, 247–250

Kylafis, N. D., Contopoulos, I., Kazanas, D., & Christodoulou, D. M., Formation and destruction of jets in X-ray binaries. 2012, *Astron. Astrophys.*, **538**, A5, DOI: 10.1051/0004-6361/201117052

Li, L.-X., Accretion Disk Torqued by a Black Hole. 2002a, *Astrophys. J.*, **567**, 463, DOI: 10.1086/338486

Li, L.-X., Toy model for the magnetic connection between a black hole and a disk. 2002b, *Phys. Rev. D*, **65**, 084047, DOI: 10.1103/PhysRevD.65.084047

Linet, B., Stationary axisymmetric electromagnetic fields in the Kerr metric. 1979, *Journal of Physics A Mathematical General*, **12**, 839, DOI: 10.1088/0305-4470/12/6/013

Liu, B. F., Mineshige, S., & Shibata, K., A Simple Model for a Magnetic Reconnection-heated Corona. 2002, *Astrophys. J., Lett.*, **572**, L173, DOI: 10.1086/341877

Miller, M. C. & Miller, J. M., The masses and spins of neutron stars and stellar-mass black holes. 2015, *Physics Reports*, **548**, 1, DOI: 10.1016/j.physrep.2014.09.003

Moderski, R., Sikora, M., & Lasota, J. P., On Black Hole Spins and Dichotomy of Quasars. 1997, in *Relativistic Jets in AGNs*, ed. M. Ostrowski, M. Sikora, G. Madejski, & M. Begelman, 110–116

Novikov, I. D. & Thorne, K. S., Astrophysics of black holes. 1973, in *Black Holes (Les Astres Occlus)*, ed. C. Dewitt & B. S. Dewitt, 343–450

Okazaki, A. T., Kato, S., & Fukue, J., Global trapped oscillations of relativistic accretion disks. 1987, *Publ. Astron. Soc. Jap.*, **39**, 457

Page, D. N. & Thorne, K. S., Disk-Accretion onto a Black Hole. Time-Averaged Structure of Accretion Disk. 1974, *Astrophys. J.*, **191**, 499, DOI: 10.1086/152990

Pasham, D. R., Cenko, S. B., Zoghbi, A., et al., Evidence for High-frequency QPOs with a 3:2 Frequency Ratio from a 5000 Solar Mass Black Hole. 2015, *Astrophys. J., Lett.*, **811**, L11, DOI: 10.1088/2041-8205/811/1/L11

Pasham, D. R., Strohmayer, T. E., & Mushotzky, R. F., A 400-solar-mass black hole in the galaxy M82. 2014, *Nature*, **513**, 74, DOI: 10.1038/nature13710

Poutanen, J., Lipunova, G., Fabrika, S., Butkevich, A. G., & Abolmasov, P., Supercritically accreting stellar mass black holes as ultraluminous X-ray sources. 2007, *Mon. Not. R. Astron. Soc.*, **377**, 1187, DOI: 10.1111/j.1365-2966.2007.11668.x

Qing, G., Wang, W., Liu, J.-F., & Yoachim, P., The Distance Measurement of NGC 1313 with Cepheids. 2015, *Astrophys. J.*, **799**, 19, DOI: 10.1088/0004-637X/799/1/19

Shakura, N. I. & Sunyaev, R. A., Black holes in binary systems. Observational appearance. 1973, *Astron. Astrophys.*, **24**, 337

Stobbart, A. M., Roberts, T. P., & Wilms, J., XMM-Newton observations of the brightest ultraluminous X-ray sources. 2006, *Mon. Not. R. Astron. Soc.*, **368**, 397, DOI: 10.1111/j.1365-2966.2006.10112.x

van der Klis, M. 2006, *Rapid X-ray Variability*, ed. W. H. G. Lewin & M. van der Klis, 39–112

Wang, D. X., Xiao, K., & Lei, W. H., Evolution characteristics of the central black hole of a magnetized accretion disc. 2002, *Mon. Not. R. Astron. Soc.*, **335**, 655, DOI: 10.1046/j.1365-8711.2002.05652.x

Wang, J.-M., Watarai, K.-Y., & Mineshige, S., The Hot Disk Corona and Magnetic Turbulence in Radio-quiet Active Galactic Nuclei: Observational Constraints. 2004, *Astrophys. J., Lett.*, **607**, L107, DOI: 10.1086/421906